diffusion limitations caused by the corrosion product obstruction.

The quantitative data acquired by the fitting of the spectra shown in Fig. 2, to the equivalent circuits, illustrated in Fig.3 are summarized in Table 1 (for three of the investigated samples). It shows only the numerical values determined at 336 and 5208 hours of exposure, since it would be onerous to represent the obtained data from all recorded spectra (all exposure times).

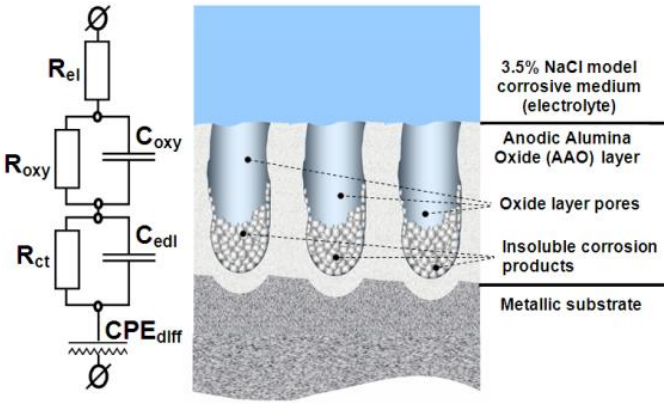

Fig. 3. Illustration of the equivalent circuit, suitable for EIS data fitting for extended exposure durations and the respective conceptual model.

Table 1. EIS data fitting results for the corrosion process kinetics

336 hours of exposure					
Element	Unit		Sample **1**	Sample **2**	Sample **3**
R_{el}	Ω cm^2		29.94 ± 2.03	95.40 ± 6.12	30.7 ± 6.32
C_{oxy}	F cm^{-2}	10^{-7}	2.67 ± 0.21	2.97 ± 0.03	3.19 ± 0.26
R_{oxy}	Ω cm^2	10^3	0.49 ± 0.04	0.204 ± 0.002	0.48 ± 0.01
C_{edl}	F cm^{-2}	10^{-7}	1.16 ± 0.01	1.36 ± 0.06	1.44 ± 0.01
R_{ct}	Ω cm^2	10^3	0.17 ± 0.03	0.46 ± 0.02	0.24 ± 0.01
Q_{diff}	s^n Ω^{-1} cm^{-2}	10^{-7}	5.91 ± 0.31	6.36 ± 0.05	6.04 ± 0.89
n	-----		0.71 ± 0.02	0.82 ± 0.03	0.84 ± 0.02
5208 hours of exposure					
Element	Unit		Sample **1**	Sample **2**	Sample **3**
R_{el}	Ω cm^2	10^3	2.44 ± 0.43	3.00 ± 0.63	2.80 ± 0.56
C_{oxy}	F cm^{-2}	10^{-9}	12.55 ± 2.88	11.78 ± 1.62	13.16 ± 1.69
R_{oxy}	Ω cm^2	10^3	163.40 ± 3.58	122.80 ± 8.65	131.40 ± 7.00
C_{edl}	F cm^{-2}	10^{-9}	3.34 ± 0.16	2.34 ± 0.10	2.58 ± 0.12
R_{ct}	Ω cm^2	10^3	63.60 ± 2.47	73.60 ± 7.21	60.80 ± 5.33
Q_{diff}	s^n Ω^{-1} cm^{-2}	10^{-7}	5.06 ± 0.10	4.88 ± 0.11	5.46 ± 0.12
n	-----		0.90 ± 0.01	0.88 ± 0.01	0.89 ± 0.01

The comparison of the data, represented in Table 1 shows that both C_{oxy} and C_{edl}, decrease by three orders of magnitude from 10^{-6} to 10^{-9} F cm^{-2}. The diffusion related constant phase element (CPE_{diff}), follows the same trend. However its coefficient (n) retains its value (around 1). This fact indicates that the CPE_{diff} resembles pure capacitance, resulting from the obstruction effect, caused by the insoluble corrosion products. Simultaneously, all the resistance elements: R_{el}, R_{oxy} and R_{ct}, increase in value, due to corrosion products accumulation. Consequently, the accumulation of polynuclear Keggin type $Al_x(OH)_{3x-z}Cl_z$ corrosion products suppresses the Al-oxide layer thinning, by hindering the access of corrosive species to the surface.

The impedance spectra components do not follow similar trends of evolution (Fig. 4).

The R_{el}, initially increases progressively, and afterwards remains unchanged at about 3 kΩ cm^2. The rest resistance components R_{oxy} and R_{edl} tend to increase linearly. This difference of the resistance evolution kinetics can be explained, having in mind that R_{el} corresponds to the total accumulation of corrosion products on the entire sample surface, whereas R_{oxy} and R_{edl} are rather related only to the corrosion product accumulation inside the AAO pores and defects.

The capacitance elements show similar trends. Initially, C_{oxy} shows a sharp decrease, followed by reaching of almost steady state at about 2 nF cm^{-2}. The C_{edl} and CPE_{diff} suffer weak linear decrease with insignificant slope.

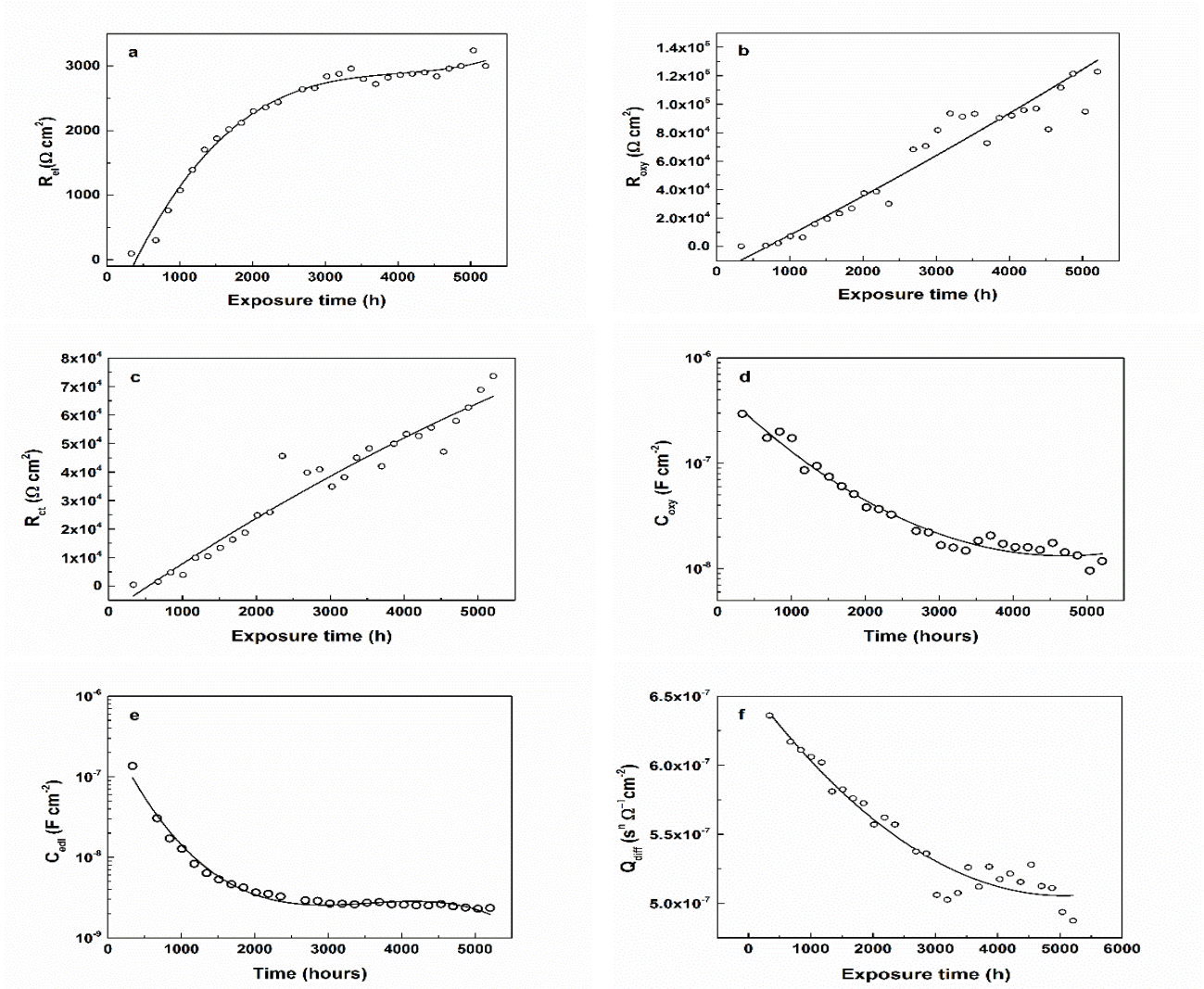

Fig. 4. Resistance (a - c), capacitance and CPE (d - f) values evolution during the exposure to the model corrosive medium

Linear sweep voltammetry

This method was used, because any eventual AAO breakdowns could easily be determined by the sharp changes of the respective LSV curves. Besides, this method enables the detection of localized corrosion activities [34], by the occurrence of sharp inflexions in the anodic LSV branches.

In the present case the LSV curves acquired even after 5208 hours of exposure to the model corrosive medium, remain at the equipment minimal current detection threshold (Fig. 5).

This fact obviously evinces the lack of any oxide film breakdowns for the entire period of exposure (5208 hours), confirming the inferences done for the EIS measurements. The LSV curves are horizontal, revealing the passivation role of the AAO formed during anodization.

Summarizing the data obtained by both electrochemical methods, it can be concluded that the corrosion process of anodized AA1050 alloy in stationary hydrodynamic conditions is a self-inhibiting process, due to the insoluble corrosion products accumulation and the consequent pore obstruction. These processes suppress the corrosion process, because of the corrosive species hindering the inside of AAO pores and defects.

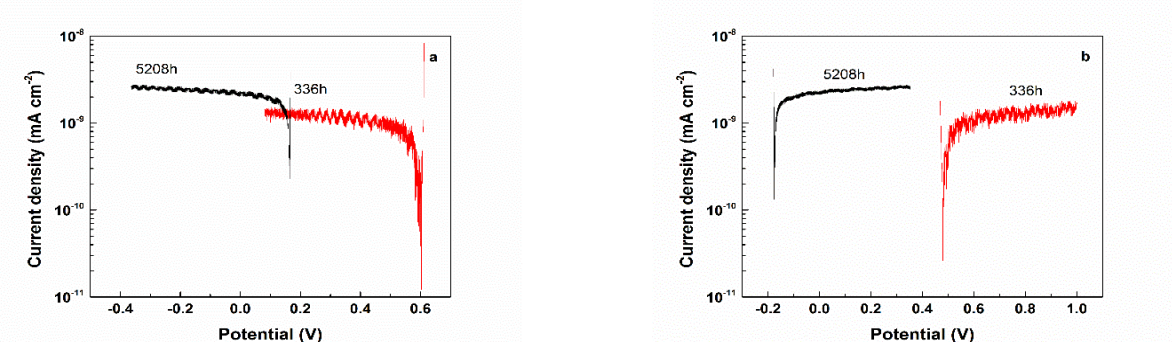

Fig. 5. Cathodic (a) and anodic (b) LSV curves, recorded for two exposure durations (336 and 5208 h)

CONCLUSIONS

The remarkable durability of Anodized Aluminum Oxide (AAO) layer grown on technically pure aluminum substrates in conventional 3.5% NaCl model corrosive medium was evaluated. The specimens did not show any remarkable indications for corrosion even after 5208 hours of exposure.

The acquired EIS spectra have shown almost pure capacitance, revealing the well-defined insulation properties of the obtained AAOs. Indeed, the phase shift approached 90 degrees. Besides, the spectra shapes changed gradually, due to lack of any film breakdowns for the entire exposure period.

A quantitative numerical analysis was applied to the acquired EIS spectra by fitting to appropriate equivalent circuits. The successful data fitting required pure capacitances (C), instead of Constant Phase Elements (CPE). This fact confirms the purely capacitive properties of the obtained AAO films. The equivalent circuit data fitting has shown that additional CPE was necessary for the data fitting of the spectra, acquired after 336 hours of exposure. This element was ascribed to pore obstruction by $Al_x(OH)_{3x-y}Cl_y$ products. The further data fitting analysis has shown gradual decrease of the capacitances, coupled by simultaneous resistance increment.

On the basis of all data, it was established that the AAO suffer gradual deterioration which decelerates with time. The reason for this deceleration is the access suppression of corrosive species, due to the pore obstruction commented above.

The LSV curves have undoubtedly confirmed the inferences done for the EIS data analysis. All the curves, acquired for the entire period of 5208 hours of exposure were at insignificant currents, approaching the equipment minimum current detection threshold. This fact confirms the statement that the AAO films are able to resist and do not suffer any breakdowns for the entire exposure period.

Acknowledgements: *The authors are grateful for the funding of this research to the Bulgarian National Scientific Research Fund, under contract DFNI-T02-27.*

REFERENCES

1. M. Lamberti, F. Escher, *Food Rev. Internat*., **23**, 407 (2007).
2. O. Ayalon, Y. Avnimelech, M. Shechter, *Envir. Sci. Pol*., **3**, 135 (2000).
3. C. C. Huang, H. W. Ma, *Sci. Total Env*., **324**, 161 (2004).
4. K. Marsh, B. Bugusu, *Mater. Envir. Iss*., **72**, R39 (2007).
5. S. P. Joshi, R. B. Toma, N. Medora, K. O'Connor, *Food Chemistry*, **83**, 383 (2003).
6. M. Šeruga, J. Grgić, M. Mandić, *Z. Lebensm. Unters.Forch.*, **198**, 313 (1994).
7. F. Bianchi, M. Careri, M. Maffini, A. Mangia, C. Mucchino, *Rapid Commun. Mass Spectr*., **17**, 251 (2003).
8. A. Becaria, A. Campbell, S. C. Bondy, *Toxicol. Ind. Health*, **18**, 309 (2002).
9. J. Kandiah, C. Kies, *Biometals*, **7**, 57 (1994).
10. S. S. Golru, M. M. Attar, B. Ramezanzadeh, *Appl. Surf. Sci*., **345**, 360 (2015).
11. S. S. Golru, M.M. Attar, B. Ramezanzadeh, *Prog. Org. Coat*., **87**, 52 (2015).
12. S. S. Golru, M.M. Attar, B. Ramezanzadeh, *J. Ind. Eng. Chem*., **24**, 233 (2015).
13. D. E. Johnson, T. L. Anderson, US patent, US6559385B1 (2003).
14. C. McCullough, A. Mortensen, P. S. Werner, H. E. Deve, T. L. Anderson, US patent US6180232B1 (1995).
15. X. Y. Huang, P. K. Jiang, J. Appl. Phys., 102, 124103 (2016).
16. C. Hiel, G. Korzeniowski, D. Bryant, US Patent US7179522B2 (2004).
17. J. Crahay, US Patent, US4322600A (1979).
18. T. M. Smith, US Patent, US3987897A (1975).
19. C. Ralph E., US Patent, US2114072A (1938).

20. J. Curt, US Patent, US2780253A (1950).
21. F. C. Chen, M. K. Chuang, S. C. Chien, J. H. Fang, C. W. Chu, *J. Mater. Chem*., **21**, 11378 (2011).
22. R. Abdel-Karim, S. M. El-Raghy, Chapter 7 in: Nanofabrication using Nanomaterials, J. Ebothé, W. Ahmed (Eds.) One Central Press (Manchester U.K.) 2016, p. 197 - 218
23. P. Vachkov, D.Ivanov, Gov. Ed. "Tekhnicka" Sofia, 15 (1990).
24. S. Iwauchi, T. Tanaka, *Jpn. J. Appl. Phys*., **10**, 260 (1971).
25. H. Klauk, *Nature Materials*, **8**, 853 (2009).
26. P. Bocchetta, M. Santamaria, F. Di Quarto, *J. Mater. Sci. Nanotehnol*., **1**, 1 (2014).
27. T. Kumeria, A. Santos, D. Losic, *Sensors*, **14**, 11878 (2014).
28. A.Santos, T. Kumeria, D. Losic, *Materials*, **7**, 4297 (2014).
29. H. Kaesche, Corrosion of the Metals, "Metallurgy" Gov. Ed., Moscow, 219 (1984).
30. M. Machkova, E.A. Matter., S. Kozhukharov, V. Kozhukharov, Corros. Sci. 69, 396 (2013).
31. S. Kozhukharov, V. Kozhukharov, M. Wittmar, M. Schem, M. Aslan, H.Caparrotti, M.Veith, *Prog. Org. Coat.*, **71**, 198 (2011).
32. A. A. Salve, S. Kozhukharov, J. E. Pernas, E. Matter, M. Machkova, *J. Univ. Chem.Technol. Metal*., **47**, 319 (2012).
33. B. A. Boukamp, *Solid State Ionics*, **18/19**, 136 (1986).
34. M. Bethencourt, F. J. Botana, J. J. Calvino, M. Marcos, M. A. Rodriguez-Chacon, *Corros. Sci.*, **40**, 1803 (1998).

КОРОЗИОННА УСТОЙЧИВОСТ НА АНОДНИ ОКСИДНИ СЛОЕВЕ (АОС) ОТЛОЖЕНИ ВЪРХУ ТЕХНИЧЕСКИ ЧИСТА СПЛАВ АА1050

К. А. Гиргинов, С. В. Кожухаров, М. Х. Миланес

Химикотехнологичен и металургичен университет, бул. Климент Охридски№8,1756 София,България

Постъпила на 03 юни 2017 г.; приета на 07 октомври 2017 г.

(Резюме)

Представени са данни за значителната корозионна устойчивост на анодни оксидни слоеве (АОС), формирани върху техническата алуминиева сплав АА1050. Формирането на оксидните филми е проведено галваностатично (15 $mAcm^{-2}$) и изотермично (20 °C) в 15% H_2SO_4, в продължениена 48 min. Процесът е провеждан с образци от АА1050 (30x30 mm) в двуелектродна електролизна клетка, при непрекъснато разбъркване на електролита. Изследванията на АОС са проведени след продължително (до 5208 часа) експониране на образците в моделна корозионна среда (3.5% NaCl). Чрез Електрохимична Импедансна Спектроскопия (ЕИС) и Линейна Волтамперометрия (ЛВА) оксидните слоеве са подлагани на регулярни (ежеседмични) електрохимични измервания. Анализът на импедансните спектри показва почти чисто капацитивно поведение на изследваните образци, което се дължи на добре изразената изолаторна способност на оксидните слоеве. Оксидните слоеве запазват своите капацитивни свойства през целия период на експозиция, демонстрирайки много добра корозионна устойчивост. Получените импедансни спектри са подложени на количествен анализ при използване на подходящи еквивалентни схеми. Резултатите получени чрез импедансните спектри за свойствата на АОС са потвърдени и от проведените волтамперометрични измервания. Регистрираните токови плътности (в анодна и катодна посока) потвърждават заключенията за почти чистото капацитивно поведение на формираните АОС. Получените данни показват, че дори след 5208 часово излагане в корозионна среда не се наблюдават забележими корозионни поражения. Това е убедително доказателство, че формираните оксидни слоеве могат ефективно да защитават алуминиевата АА1050 сплав.

Ключови думи: Анодиране, Анодни филми върху алуминий, ЕИС, ЛСВ